Available online at www.sciencedirect.com
SCIENCE DIRECT
Journal of Sound and Vibration 294 (2006) 1016–1038
JOURNAL OF SOUND AND VIBRATION
www.elsevier.com/locate/jsvi

Free vibration of simply supported functionally graded and layered magneto-electro-elastic plates by finite element method

Rajesh K. Bhangale, N. Ganesan*

Machine Design Section, Department of Mechanical Engineering, Indian Institute of Technology Madras, Chennai 600 036, India

Received 24 August 2005; received in revised form 7 December 2005; accepted 22 December 2005
Available online 28 February 2006

Abstract

In this article, free vibration studies on functionally graded, anisotropic and linear magneto-electro-elastic plates have been carried out by semi-analytical finite element method. A series solution is assumed in the plane of the plate and finite element procedure is adopted across the thickness of the plate such a way that the three-dimensional (3-D) character of the solution is preserved. The finite element model is derived based on constitutive equation of magneto-electro-elastic material accounting for coupling between elasticity, electric and magnetic effect. The present finite element is modeled with displacement components, electric potential and magnetic potential as nodal degree of freedom. The functionally graded material is assumed to be exponential in the thickness direction. The numerical results obtained by the present model are in good agreement with the isotropic 3-D exact benchmark solutions available in literature. Numerical study includes the influence of the different exponential factor, magneto-electro-elastic properties and effect of mechanical and electrical type of loading on induced magneto-electro-elastic fields. Further study has been carried out on higher harmonic. Study has been extended on functionally graded and layered magneto-electro-elastic plate.

1. Introduction

Literature dealing with research on the behavior of magneto-electro-elastic structures has gained more importance recently as these smart materials have the ability of converting energy from one form to the other (among magnetic, electric and mechanical energy) [1,2]. Such materials can exhibit field coupling that is not present in any of the monolithic constituent material. With application in ultrasonic imaging devices, sensors, actuators, transducers and many other emerging components, there is a strong need for theories or techniques that can predict the coupled response of these so-called smart materials, as well as structure composed of them. Studies on static and dynamic behavior on plates as well as infinite cylinder has been dealt in literature. Pan [3] derived an exact closed-form solution for the simply supported and multilayered plate made of anisotropic piezoelectric and piezomagnatic materials under a static mechanical load. Pan and Heyliger [4] solved the corresponding vibration problem. Piezoelectric and piezomagnetic composites exhibit coupling effect of electric and magnetic fields. In most of the studies, these composite materials have been used as layers

*Corresponding author. Tel.: +91 44 2351365; fax: +91 44 2350509.
E-mail addresses: rajesh_phd@iitm.ac.in (R.K. Bhangale), nganesan@iitm.ac.in (N. Ganesan).

0022-460X/$ - see front matter © 2006 Elsevier Ltd. All rights reserved.
doi:10.1016/j.jsv.2005.12.030

or as multiphase. The behavior of finitely long cylindrical shells under uniform internal pressure has been studied by Wang and Zhong [5] and they concluded that piezoelectric and piezomagnetic composites in general have the coupling effect, which is two orders higher than that of single-phase magnetoelctric constituent materials. Micro-mechanical analysis of fully coupled electro-magneto-thermo-elastic composites has been carried out by Aboudi [6] for the prediction of the effective moduli of magneto-electro-elastic composites. Li [7] studied the multi-inclusion and inhomogenity problems in a magneto-electro-elastic solid. Wang et al. [8] derived the state vector approach to analysis of multilayered magneto-electro-elastic plates for mechanical and electrical loading.

From the literature survey, it is found that only few studies have been reported on magneto-electro-elastic structures by finite element analysis. Free vibration behavior of infinitely long magneto-electro-elastic cylindrical shell has been studied by Buchanan [9] by using semi-analytical finite element method. Buchanan [10] has studied the behavior of layered versus multiphase magneto-electro-elastic infinite long plate composites by finite element method. Lage et al. [11] developed a layerwise partial mixed finite element model for static analysis of magneto-electro-elastic plate. Most recently, authors [12,13] proposed the 3-D finite element analysis for FGM cylindrical shells. In addition, authors [14] carried out static analysis of FGM magneto-electro-elastic plate by finite element method under mechanical and electrical loading.

The special feature of graded spatial compositions (non-homogeneous) associated with FGM provides freedom in the design and manufacturing of novel structures. Still there are great challenges in the numerical modeling and simulation of the FGM structure [15–18]. The studies on non-homogeneous magneto-electro-elastic structure are less in literature. Chen and Lee [19] adopted state-space formulation to derive equations for non-homogeneous transversely isotropic magneto-electro-elastic plates. Chen et al. [20] carried out free vibration analysis of non-homogeneous transversely isotropic magneto-electro-elastic plates. Pan and Han [21] presented an exact solution for functionally graded and layered magneto-electro-elastic plates by pseudo-Stroh formalism.

It appears from literature survey that there is no finite element formulation available for vibration studies on finite FGM and layered magneto-electro-elastic plate. Hence, in present study, free vibration analysis of FGM and layered magneto-electro-elastic plates has been carried out by using series solution in conjunction with finite element approach. The main aim of the study is to bring out effects of piezo-electric, magnetostrictive and coupling terms on frequency behavior, categorically through proposed five classes of vibration. In addition, this study has been dealt on higher harmonic too. Further study has been extended on FGM layered with thickness to span ratio subjected to open and closed circuit electric boundary condition.

2. Basic equations

The coupled constitutive equations for anisotropic and linearly magneto-electro-elastic solids can be written as

$$\sigma_j = C_{jk}S_k - e_{kj}E_k - q_{kj}H_k, \tag{1}$$

$$D_j = e_{jk}S_k + \varepsilon_{jk}E_k + m_{jk}H_k, \tag{2}$$

$$B_j = q_{jk}S_k + m_{jk}E_k + \mu_{jk}H_k, \tag{3}$$

where σ_j denotes stress, D_j is electric displacement and B_j is magnetic induction. C_{jk}, ε_{jk} and μ_{jk} are the elastic, dielectric and magnetic permeability coefficients. e_{kj}, q_{kj} and m_{jk} are piezoelectric, piezomagnetic and magnetoelectric material coefficients. Apparently, various uncoupled cases can be reduced from Eqs. (1)–(3). A completely coupled magneto-electro-elastic material matrix, assuming a hexagonal crystal class, for above

constitutive equations is given below by Buchanan [10]:

$$\begin{Bmatrix} \sigma_1 \\ \sigma_2 \\ \sigma_3 \\ \sigma_4 \\ \sigma_5 \\ \sigma_6 \\ D_1 \\ D_2 \\ D_3 \\ B_1 \\ B_2 \\ B_3 \end{Bmatrix} = \begin{bmatrix} C_{11} & C_{12} & C_{13} & 0 & 0 & 0 & 0 & 0 & e_{31} & 0 & 0 & q_{31} \\ C_{12} & C_{11} & C_{13} & 0 & 0 & 0 & 0 & 0 & e_{31} & 0 & 0 & q_{31} \\ C_{13} & C_{13} & C_{33} & 0 & 0 & 0 & 0 & 0 & e_{33} & 0 & 0 & q_{33} \\ 0 & 0 & 0 & C_{44} & 0 & 0 & 0 & e_{15} & 0 & 0 & q_{15} & 0 \\ 0 & 0 & 0 & 0 & C_{44} & 0 & e_{15} & 0 & 0 & q_{15} & 0 & 0 \\ 0 & 0 & 0 & 0 & 0 & C_{66} & 0 & 0 & 0 & 0 & 0 & 0 \\ 0 & 0 & 0 & 0 & e_{15} & 0 & \varepsilon_{11} & 0 & 0 & m_{11} & 0 & 0 \\ 0 & 0 & 0 & e_{15} & 0 & 0 & 0 & \varepsilon_{11} & 0 & 0 & m_{11} & 0 \\ e_{31} & e_{31} & e_{33} & 0 & 0 & 0 & 0 & 0 & \varepsilon_{33} & 0 & 0 & m_{33} \\ 0 & 0 & 0 & 0 & q_{15} & 0 & m_{11} & 0 & 0 & \mu_{11} & 0 & 0 \\ 0 & 0 & 0 & q_{15} & 0 & 0 & 0 & m_{11} & 0 & 0 & \mu_{11} & 0 \\ q_{31} & q_{31} & q_{33} & 0 & 0 & 0 & 0 & 0 & m_{33} & 0 & 0 & \mu_{33} \end{bmatrix} \begin{Bmatrix} S_1 \\ S_2 \\ S_3 \\ S_4 \\ S_5 \\ S_6 \\ E_1 \\ E_2 \\ E_3 \\ H_1 \\ H_2 \\ H_3 \end{Bmatrix} \tag{4}$$

The strain displacement relations are

$$S_{xx} = S_1 = \frac{\partial u}{\partial x}, \quad S_{yy} = S_2 = \frac{\partial v}{\partial y}, \quad S_{zz} = S_3 = \frac{\partial w}{\partial z},$$

$$S_{yz} = S_4 = \frac{\partial v}{\partial z} + \frac{\partial w}{\partial y}, \quad S_{xz} = S_5 = \frac{\partial u}{\partial z} + \frac{\partial w}{\partial x}, \quad S_{xy} = S_6 = \frac{\partial u}{\partial y} + \frac{\partial v}{\partial x}, \tag{5}$$

where u, v and w are mechanical displacements in co-ordinate directions x, y and z.

The electric field vector E_i is related to the electric potential ϕ as follows:

$$E_x = E_1 = -\frac{\partial \phi}{\partial x}, \quad E_y = E_2 = -\frac{\partial \phi}{\partial y}, \quad E_z = E_3 = -\frac{\partial \phi}{\partial z}. \tag{6}$$

The magnetic field H_i is related to magnetic potential Ψ as follows:

$$H_x = H_1 = -\frac{\partial \psi}{\partial x}, \quad H_y = H_2 = -\frac{\partial \psi}{\partial y}, \quad H_z = H_3 = -\frac{\partial \psi}{\partial z}. \tag{7}$$

3. Finite element formulation

Recently, authors [14] have analyzed static studies on functionally graded and layered plate. In the present work, finite series solution has been assumed satisfying boundary conditions for simply supported plates has been adopted. The finite element model has been used in the thickness direction. For a general loading, the shape functions are as follows:

$$u(x,y,z) = \sum_{n=1}^{N}\sum_{m=1}^{M} U_{nm}(z)\cos\left(\frac{n\pi}{L_x}\right)x\,\sin\left(\frac{m\pi}{L_y}\right)y,$$

$$v(x,y,z) = \sum_{n=1}^{N}\sum_{m=1}^{M} V_{nm}(z)\sin\left(\frac{n\pi}{L_x}\right)x\,\cos\left(\frac{m\pi}{L_y}\right)y,$$

$$w(x,y,z) = \sum_{n=1}^{N}\sum_{m=1}^{M} W_{nm}(z)\sin\left(\frac{n\pi}{L_x}\right)x\,\sin\left(\frac{m\pi}{L_y}\right)y,$$

$$\varphi(x,y,z)=\sum_{n=1}^{N}\sum_{m=1}^{M}\Phi_{nm}(z)\sin\left(\frac{n\pi}{L_x}\right)x\,\sin\left(\frac{m\pi}{L_y}\right)y,$$
$$\psi(x,y,z)=\sum_{n=1}^{N}\sum_{m=1}^{M}\Psi_{nm}(z)\sin\left(\frac{n\pi}{L_x}\right)x\,\sin\left(\frac{m\pi}{L_y}\right)y, \tag{8}$$

where n and m being two positive integers and N and M are the number of terms in the series to be accounted for the general loading. In the present study, analysis has been carried out similar to that reported by Pan and Han [21] for $m=n=1$. In the end, the analysis has been reduced for finite element in the thickness direction, still retaining the 3-D dependence of the solution based on the choice of n and m. The analysis is carried out by two-noded finite element and the assumed shape functions are

$$U_i=[N_u]\{U\},\quad \Phi=[N_\varphi]\{\Phi\},\quad \Psi=[N_\varphi]\{\Psi\}, \tag{9}$$

where

$$N_1=\left(1-\frac{z_i}{z_{i+1}-z_i}\right),\quad N_2=\left(\frac{z_i}{z_{i+1}-z_i}\right).$$

For a coupled filed problem, finite element equations are as follows:

$$[[K_{uu}]-\omega^2[M]]\{U\}+[K_{u\phi}]\{\phi\}+[K_{u\psi}]\{\psi\}=0,$$

$$[K_{u\phi}]^{\mathrm{T}}\{U\}-[K_{\phi\phi}]\{\phi\}-[K_{\phi\psi}]\{\psi\}=0,$$

$$[K_{u\psi}]^{\mathrm{T}}\{U\}-[K_{\phi\psi}]^{\mathrm{T}}\{\phi\}-[K_{\psi\psi}]\{\psi\}=0. \tag{10}$$

Various stiffness matrices are defined as follows:

$$[K_{uu}]=c\int[B_u]^{\mathrm{T}}[C][B_u]\,\mathrm{d}z,\quad [K_{u\phi}]=c\int[B_u]^{\mathrm{T}}[e][B_\phi]\,\mathrm{d}z,\quad [K_{u\psi}]=c\int[B_u]^{\mathrm{T}}[q][B_\psi]\,\mathrm{d}z,$$

$$[K_{\phi\phi}]=c\int[B_\phi]^{\mathrm{T}}[\varepsilon][B_\phi]\,\mathrm{d}z,\quad [K_{\psi\psi}]=c\int[B_\psi]^{\mathrm{T}}[\mu][B_\psi]\,\mathrm{d}z,\quad [K_{\phi\psi}]=c\int[B_\phi]^{\mathrm{T}}[m][B_\psi]\,\mathrm{d}z, \tag{11}$$

where $C=0.25L_xL_y$ and $[B_u]$, $[B_\phi]$, $[B_\psi]$ represents the strain-displacement, electric field–electric potential and magnetic field–magnetic potential relations, respectively. The component matrices for Eq. (11) are

$$[B_u]=[L_u][N_u]=\begin{bmatrix}\frac{\partial}{\partial x}&0&0\\0&\frac{\partial}{\partial y}&0\\0&0&\frac{\partial}{\partial z}\\0&\frac{\partial}{\partial z}&\frac{\partial}{\partial y}\\\frac{\partial}{\partial z}&0&\frac{\partial}{\partial x}\\\frac{\partial}{\partial y}&\frac{\partial}{\partial x}&0\end{bmatrix}\begin{bmatrix}N_1&0&0&N_2&0&0\\0&N_1&0&0&N_2&0\\0&0&N_1&0&0&N_2\end{bmatrix}, \tag{12}$$

$$[B_u] = \begin{bmatrix} -\left(\frac{n\pi}{L_x}\right)N_1 & 0 & 0 & \ldots \\ 0 & -\left(\frac{m\pi}{L_x}\right)N_1 & 0 & \ldots \\ 0 & 0 & \frac{\partial N_1}{\partial z} & \ldots \\ 0 & \frac{\partial N_1}{\partial z} & \left(\frac{m\pi}{L_x}\right)N_1 & \ldots \\ \frac{\partial N_1}{\partial z} & 0 & \left(\frac{n\pi}{L_x}\right)N_1 & \ldots \\ \left(\frac{m\pi}{L_x}\right)N_1 & \left(\frac{n\pi}{L_x}\right)N_1 & 0 & \ldots \end{bmatrix}, \tag{13}$$

where there are three additional columns for N_2. The matrix $[B_\phi]$ is developed using Eq. (6) and is as follows:

$$[B_\phi] = [L_\phi][N_\phi] = \begin{bmatrix} \frac{\partial}{\partial x} \\ \frac{\partial}{\partial y} \\ \frac{\partial}{\partial z} \end{bmatrix} \begin{bmatrix} N_1 & N_2 \end{bmatrix} = \begin{bmatrix} -\left(\frac{n\pi}{L_x}\right)N_1 & -\left(\frac{n\pi}{L_x}\right)N_2 \\ -\left(\frac{m\pi}{L_y}\right)N_1 & -\left(\frac{m\pi}{L_y}\right)N_2 \\ \frac{\partial N_1}{\partial z} & \frac{\partial N_2}{\partial z} \end{bmatrix}. \tag{14}$$

Similarly, using Eq. (7) gives

$$[B_\psi] = [L_\psi][N_\psi] = \begin{bmatrix} \frac{\partial}{\partial x} \\ \frac{\partial}{\partial y} \\ \frac{\partial}{\partial z} \end{bmatrix} \begin{bmatrix} N_1 & N_2 \end{bmatrix} = \begin{bmatrix} -\left(\frac{n\pi}{L_x}\right)N_1 & -\left(\frac{n\pi}{L_x}\right)N_2 \\ -\left(\frac{m\pi}{L_y}\right)N_1 & -\left(\frac{m\pi}{L_y}\right)N_2 \\ \frac{\partial N_1}{\partial z} & \frac{\partial N_2}{\partial z} \end{bmatrix}. \tag{15}$$

In Eq. (10), by eliminating electric and magnetic potential terms by condensation techniques we get K_{eq}

$$[K_{\text{eq}}]\{U\} + [M]\{\ddot{U}\} = 0, \tag{16}$$

where

$$[K_{\text{eq}}] = [K_{uu}] + [K_{u\phi}][K_{II}]^{-1}[K_I] + [K_{u\psi}][K_V]^{-1}[K_{IV}].$$

The component matrices for Eq. (16) are

$$[K_I] = [K_{u\phi}]^{\text{T}} - [K_{\phi\psi}][K_{\psi\psi}]^{-1}[K_{u\psi}]^{\text{T}}, \tag{17}$$

$$[K_{II}] = [K_{\phi\phi}] - [K_{\phi\psi}][K_{\psi\psi}]^{-1}[K_{\phi\psi}]^{\text{T}}, \tag{18}$$

$$[K_{IV}] = [K_{u\psi}]^{\text{T}} - [K_{\phi\psi}]^{\text{T}}[K_{\phi\phi}]^{-1}[K_{u\phi}]^{\text{T}}, \tag{19}$$

$$[K_V] = [K_{\psi\psi}] - [K_{\phi\psi}]^{\text{T}}[K_{\phi\phi}]^{-1}[K_{\phi\psi}]. \tag{20}$$

The eigenvectors that correspond to the distribution of $\{\phi\}$ and $\{\psi\}$ can be as follows:

$$\phi = [K_{II}]^{-1}[K_I]\{U\}, \tag{21}$$

$$\psi = [K_V]^{-1}[K_{IV}]\{U\}. \tag{22}$$

To study the piezoelectric effect on frequency due to $BaTiO_3$ material, the stiffness matrix $[K_{eq\_\phi\phi}]$ is derived and is given by

$$[K_{eq\_\phi\phi}] = [K_{uu}] + [K_{u\phi}][K_{\phi\phi}]^{-1}[K_{u\phi}]^{T}. \tag{23}$$

To study the magnetic effect on frequency due to magnetic $CoFe_2O_4$ material, $[K_{eq\_\psi\psi}]$ is used as stiffness matrix and is as follows:

$$[K_{eq\_\psi\psi}] = [K_{uu}] + [K_{u\psi}][K_{\psi\psi}]^{-1}[K_{u\psi}]^{T}. \tag{24}$$

Material properties of homogeneous $BaTiO_3$ and $CoFe_2O_4$ are given in Appendix. In the present study, the Gaussian integration scheme has been implemented to evaluate integrals involved in different matrices, and the functionally graded material properties accounted by evaluating the material properties at Gaussian points. Different corresponding stiffness matrices have been used along with conventional mass matrix to evaluate the frequencies of the system. Present study considers around 99 elements across the thickness direction. Numerical investigation shows that the present method converges rapidly and very accuratly.

4. Analytical model of FGM material properties

4.1. Functionally graded (non-homogeneous) magneto-electro-elastic plate

First to start, study has been carried out for non-homogeneous transversely isotropic FGM magneto-electro-elastic plate reported in literature [13,21]. The present study considers functionally graded material composed of piezoelectric and magnetostrictive material. The grading is accounted across the thickness of the FGM magneto-electro-elastic plate as shown in Fig. 1(a). An advantage of a plate made of an FGM over a laminated plate is that material properties vary continuously in an FGM, while discontinuous across the adjoining layers in a laminated plate. This has been achieved by grading the volume fraction of particular material governed by power-law index. Fig. 1(b) depicts the through-the-thickness distribution of the volume

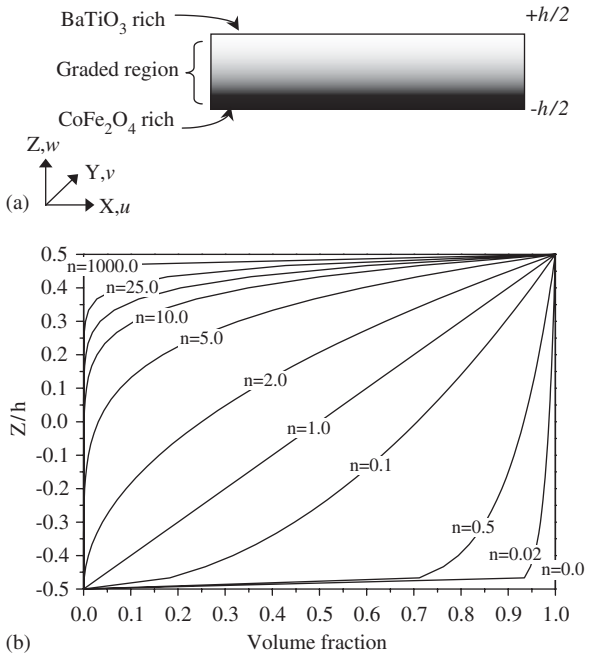

Fig. 1. (a) Coordinate and configuration of functionally graded magneto-electro-elastic plate (Model-I). (b) Through the thickness distribution of the volume fraction for different values of the power-law index n.

fraction for different power-law indices n. Consider an FGM magneto-electro-elastic plate having horizontal dimensions L_x and $L_y = 1\,\text{m} \times 1\,\text{m}$ and thickness $h = .3$. In the present analysis, it is assumed that the composition is varied from the bottom surfaces to top surface, i.e., the top surface of the plate is piezoelectric-rich, whereas the bottom surface is magnetostrictive-rich. In addition, material properties are graded throughout the thickness direction according to volume fraction power-law distribution.

The present study considers smooth and continuous variation of the volume fraction of either piezoelectric or magnetostrictive material governed by the power-law index.

A simple power-law-type definition for the volume fraction of the metal across the thickness direction of the FGM plate is assumed as

$$V_B = \left(\frac{2z+h}{2h}\right)^n, \tag{25}$$

where h is the thickness of the plate, z the thickness coordinates ($0 \leqslant z \leqslant h$), and n the power-law index. The bottom surface of the plate ($z = -h/2$) is $CoFe_2O_4$-rich, whereas the top surface ($z = h/2$) of the plate is $BaTiO_3$-rich. The sum total volume of the constituent materials, $BaTiO_3$ (B) and $CoFe_2O_4$ (F) should be

$$V_B + V_C = 1. \tag{26}$$

On the basis of the volume fraction definition and law of mixtures, the effective material property definition is as follows:

$$(\text{MP})_{\text{eff}} = (\text{MP})_{\text{top}} V_B + (\text{MP})_{\text{bottom}} V_C. \tag{27}$$

'MP' is general notation for material property. By making use of Eqs. (25)–(27), the following effective elastic, piezoelectric, piezomagnetic, dielectric and magnetic permeability, and thermal properties definitions can be written as

$$C_{\text{eff}} = (C_B - C_F)\left(\frac{2z+h}{2h}\right)^n + C_F, \tag{28a}$$

$$e_{\text{eff}} = (e_B - e_F)\left(\frac{2z+h}{2h}\right)^n + e_F, \tag{28b}$$

$$q_{\text{eff}} = (q_B - q_F)\left(\frac{2z+h}{2h}\right)^n + q_F, \tag{28c}$$

$$\varepsilon_{\text{eff}} = (\varepsilon_B - \varepsilon_F)\left(\frac{2z+h}{2h}\right)^n + \varepsilon_F, \tag{28d}$$

$$\mu_{\text{eff}} = (\mu_B - \mu_F)\left(\frac{2z+h}{2h}\right)^n + \mu_F. \tag{28e}$$

In the above Eqs. (28a)–(28e), 'eff' stands for effective material properties obtained by the above equations for particular power-law index n. Material coefficients of the piezoelectric $BaTiO_3$ and magnetostrictive $CoFe_2O_4$ is given in Appendix. In addition, variation of effective dielectric coefficients and effective magnetic permeability with respect to power-law index n across the thickness direction is shown in Fig. 2(a) and (b). It is seen that for power-law index $n = 1.0$ the variation of effective material property is linear.

4.2. Functionally graded and layered magneto-electro-elastic plate (Model-II)

Further study has been carried out on functionally graded and layered FGM plate (Model-II) made up of three layers considered as reported in literature [14–21]. The there layers have equal thickness of .1 m and the horizontal dimensions of the plate are $L_x \times L_y = 1\,\text{m} \times 1\,\text{m}$. Two functionally graded and layered sandwich plates with stacking sequences $BaTiO_3/COFe_2O_4/BaTiO_3$ ($B/F/B$) and $CoFe_2O_4/BaTiO_3/COFe_2O_4$ ($F/B/F$) are shown in Fig. 3(a). Both top and bottom layers are functionally graded with the symmetric exponential

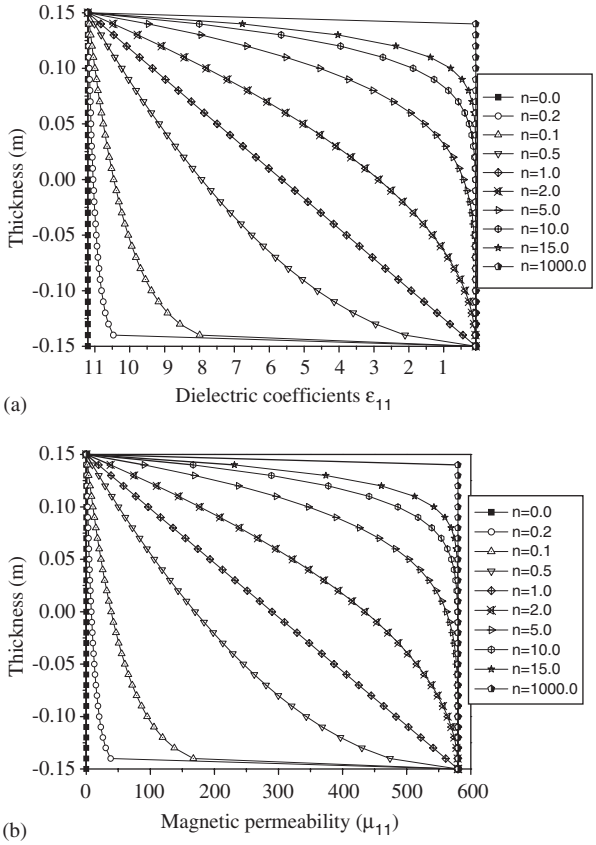

Fig. 2. (a) Variations of effective dielectric constants of magnetostrictive material along the thickness direction of functionally graded plate (Model-I). (b) Variations of effective magnetic permeability constants of magnetostrictive material along the thickness direction of functionally graded plate (Model-I).

variation as shown in Fig. 3(b). Five different exponential factors, i.e., $\eta = -10, -5, 0, 5, 10\,(1/\mathrm{m})$, were studied.

For the functionally graded material with exponential variation in the thickness direction (z-direction), the material coefficients are given by

$$C_{ik}(z) = C^0_{ik}e^{\eta z}, \quad e_{ik}(z) = e^0_{ik}e^{\eta z}, \quad q_{ik}(z) = q^0_{ik}e^{\eta z},$$
$$\varepsilon_{ik}(z) = \varepsilon^0_{ik}e^{\eta z}, \quad \mu_{ik}(z) = \mu^0_{ik}e^{\eta z}, \quad d_{ik}(z) = d^0_{ik}e^{\eta z}, \tag{29}$$

where η is the exponential factor governing the degree of the material gradient in the z-direction, and the superscript 0 is attached to indicate the z-independent factors in the material coefficients; $\eta = 0$ corresponds to the homogeneous material case.

5. Result and discussion

The present section devotes on frequency behavior of both FGM models under the influence of power-law index, different thickness to span ratio and open and closed circuit boundary condition by using finite element formulation. To check the accuracy of the proposed finite element, the code has been verified with various benchmark solutions available in literature. First, a benchmark problem [4] is considered for validation for isotropic magneto-electro-elastic plate. Secondly, validation is carried out with another benchmark solution carried out [20] for non-homogeneous transversely isotropic magneto-electro-elastic plate. A further study has been carried out on different exponential factors, and effect of magneto-electro-elastic

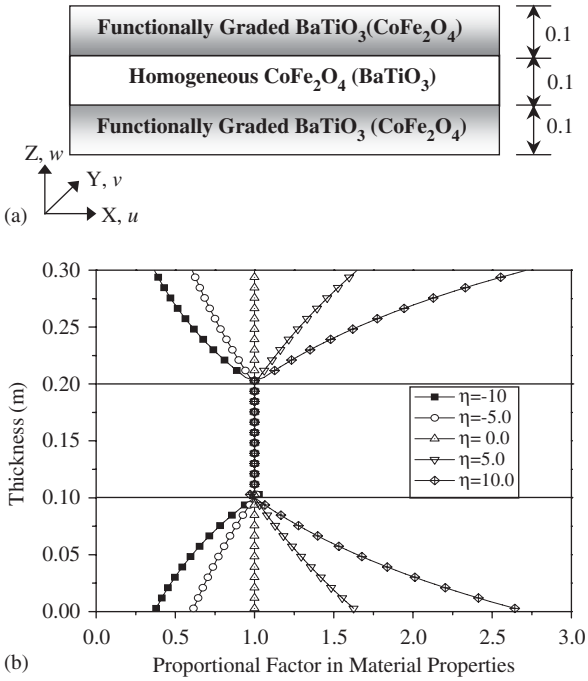

Fig. 3. (a) Coordinate and configuration of functionally graded and layered magneto-electro-elastic plate under study (Model-II). (b) Variation of FGM proportional coefficient ($e^{\eta z}$) across the thickness of the FGM and layered plate (Model-II).

Table 1
Different class of vibration considered in present study

Class of vibration	Corresponding matrix used	Frequency
I	$[K_{uu}]$	Related to elastic property of the structure only
II	$[K_{\text{eq}}]$	Accounting coupling among magneto-electro-elastic field
III	$[K_{\text{eq\_reduced}}]$	Neglecting magneto-electric coupling
IV	$[K_{\psi\psi}]$	Considering magnetostrictive field only
V	$[K_{\phi\phi}]$	Considering piezoelectric field only

coupling has been explained with mode shapes. In addition, studies have been extended for higher harmonic too. Densities of both materials are assumed to be same. As mentioned earlier, five different classes of vibration are brought out and the corresponding terminology used in the subsequent result and discussion are given in Table 1.

5.1. Validation

A square plate of $h/L_x = h/L_y = 1$ studied by Pan and Heyliger [4] is considered here for comparison. Table 2 shows the frequency parameter $\omega^* = \omega L_x\sqrt{C_{\max}/\rho_{\max}}$ for the I and II classes of vibration. Pan and Heyliger [4] reports the lowest frequency of the I class of vibration which is evidenced by looking at the mode shapes of mode 1 of the B only plate in their work. An excellent correlation has been observed for mode 1. Please note that our finite element results are identical with Ref. [4] calculation of the B, F, and different stacking sequences of $B/F/B$ and $F/B/F$. However, discrepancy around 3% is observed for other higher modes. Similar conclusion was also reported by Chen et al. [20]. Further results have been verified with Chen et al. [20] for both the I as well as II class of the vibration. It is seen that the present finite element gives an

Table 2
Frequency parameter $\omega^* = \omega L_x\sqrt{C_{\max}/\rho_{\max}}$ (open circuit) in sandwich piezoelectric and magnetostrictive plate studied by Pan and Heylinger [4] and Chen et al. [20]

Order	$BaTiO_3$ (B)		$CoFe_2O_4$ (F)	
	I	II	I	II
1	2.30033	2.10913	1.97472	1.5403
2	2.80149	2.81531	2.33729	2.33729
3	3.93970	3.96147	3.18632	3.18663
4	5.32145	4.38882	424020	3.79138
5	6.80079	5.50712	538002	4.53427
Order	$B/F/B$		$F/B/F$	
	I	II	I	II
1	1.82466	1.54741	1.89864	1.60583
2	2.15576	2.15576	2.31552	2.24953
3	3.07673	3.08466	3.11597	3.22766
4	4.11595	3.44441	4.17799	3.74352
5	5.25651	4.39337	5.30974	4.39879

Table 3
Normalized natural frequency for power-law index $n = .0$ piezoelectric (B only) plate

Mode number	Class of vibration				
	I	II	III	IV	V
1	1.9180	2.1091	2.1091	1.9180	2.1091
2	*2.3003*	*2.3003*	*2.3003*	*2.3003*	*2.3003*
3	2.6503	*2.8014*	*2.8014*	2.6503	*2.8014*
4	*2.8014*	2.8153	2.8153	*2.8014*	2.8153
5	3.7772	*3.9397*	*3.9397*	3.7772	*3.9397*
6	*3.9397*	3.9614	3.9614	*3.9397*	3.9614
7	4.2646	4.3888	4.3888	4.2646	4.3888
8	*5.3214*	*5.3214*	*5.3214*	*5.3214*	*5.3214*
9	5.3370	5.5071	5.5071	5.3370	5.5071
10	5.3787	5.5547	5.5547	5.3787	5.5547
11	*6.8007*	*6.8007*	*6.8007*	*6.8007*	6.8007

excellent correlation with analytical results given in Ref. [20]. In addition, code has been verified for results available in literature for elastic and piezoelectric plate by setting e_{ij} or q_{ij}, or both equal to zero.

5.2. Numerical studies on FGM (I) plate for different power-law index

Frequency analysis of FGM plate has been carried out for $m = n = 1$, which represents the fundamental vibration mode of the practical importance. In order to understand the influence of the piezoelectric and piezomagnetic material, five different classes of vibration are studied for all the first 11 modes and reported in Tables 3–7. Different corresponding stiffness matrices have been used along with conventional mass matrix to evaluate the frequencies of the system. Tables 3–7 gives the normalized frequency obtained by including elastic, piezoelectric effect, piezomagnetic effect and combination effect for all modes including bending as well as inplane for different power-law index as $n = 0$, .2, 1.0, 5.0 and 1000.0. Here, power-law index $n = .0$ corresponding to an isotropic plate with properties corresponds to that of homogeneous $BaTiO_3$

Table 4
Normalized natural frequency for power-law index $n = .2$ of FGM plate

Mode number	Class of vibration				
	I	II	III	IV	V
1	1.9211	2.08945	2.08945	1.91978	2.09049
2	2.3216	2.32164	2.32164	2.32164	2.32164
3	2.6712	2.81708	2.81708	2.67089	2.81721
4	2.8177	2.81777	2.81777	2.81777	2.81777
5	3.8076	3.93875	3.93875	3.80708	3.93875
6	3.9387	3.96729	3.96729	3.93875	3.96994
7	4.3628	4.48349	4.48349	4.36155	4.48543
8	5.3070	5.30702	5.30702	5.30702	5.30702
9	5.3981	5.56001	5.56001	5.39618	5.56489
10	5.5095	5.61852	5.61852	5.50444	5.62060
11	6.7746	6.77464	6.77464	6.77464	6.77464

Table 5
Normalized natural frequency for power-law index $n = 1.0$ of FGM plate

Mode number	Class of vibration				
	I	II	III	IV	V
1	1.89464	1.98968	1.98968	1.89014	1.99376
2	2.33942	2.33942	2.33942	2.33942	2.33942
3	2.69344	2.77998	2.77998	2.69247	2.78071
4	2.81704	2.81704	2.81704	2.81704	2.81704
5	3.82367	3.89045	3.89045	3.82309	3.89045
6	3.89045	3.92602	3.92602	3.89045	3.92693
7	4.46267	4.55060	4.55060	4.46406	4.54812
8	5.21328	5.21328	5.21328	5.21328	5.21328
9	5.43196	5.52448	5.52448	5.43211	5.52404
10	5.77390	5.81611	5.81611	5.76817	5.82039
11	6.63754	6.63754	6.63754	6.63754	6.63754

Table 6
Normalized natural frequency for power-law index $n = 5.0$ of FGM plate

Mode number	Class of vibration				
	I	II	III	IV	V
1	1.73467	1.74004	1.74004	1.72695	1.74769
2	2.20267	2.20267	2.20267	2.20267	2.20267
3	2.53548	2.54305	2.54305	2.53399	2.54447
4	2.60829	2.60829	2.60829	2.60829	2.60829
5	3.57426	3.57426	3.57426	3.57426	3.57426
6	3.59226	3.61203	3.61203	3.59132	3.61297
7	4.20171	4.23395	4.23395	4.20536	4.22931
8	4.76377	4.76377	4.76377	4.76377	4.76377
9	5.05416	5.08377	5.08377	5.05309	5.08453
10	5.64154	5.64551	5.64551	5.64173	5.64507
11	6.04862	6.04862	6.04862	6.04862	6.04862

Table 7
Normalized natural frequency for power-law index $n = 1000.0$ (homogeneous magnetostrictive F only)

Mode number	Class of vibration				
	I	II	III	IV	V
1[b]	1.5477	1.5403	1.5403	1.5403	1.5477
2[i]	1.9747	1.9747	1.9747	1.9747	1.9747
3[b]	2.2607	2.2594	2.2594	2.2594	2.2607
4[i]	2.3372	2.3372	2.3372	2.3372	2.3372
5[i]	3.1866	3.1866	3.1866	3.1866	3.1866
6[b]	3.2202	3.2194	3.2194	3.2194	3.2202
7[b]	3.7866	3.7913	3.7913	3.7913	3.7866
8[i]	4.2402	4.2402	4.2402	4.2402	4.2402
9[b]	4.5355	4.5342	4.5342	4.5342	4.5355
10[b]	5.0571	5.0613	5.0613	5.0613	5.0571
11[i]	5.3800	5.3800	5.3800	5.3800	5.3800

'b' = bending; 'i' = inplane.

(piezoelectric) plate and $n = 1000.0$ corresponds to isotropic plate made up of magnetostrictive material ($CoFe_2O_4$). The power-law index value n other than two extreme values governs the distribution of properties of piezo-magnetic mixture in FGM plate. Variation of the composition of piezoelectric and magnetostrictive is linear for power-law index $n = 1.0$.

It is interesting to note that among five of the natural frequencies, three symmetric and two asymmetric are the same for all power-law index. In fact, these frequencies belong to I class of vibration, which accounts only elastic properties of the system. It is seen that certain vibration modes in the II class of vibration are insensitive to the magneto-electro-elastic coupling given in I class. There are certain uncoupled elastic modes existing where one has to check the effect of coupling. In order to understand the effect of coupling on frequency behavior, mode shape is plotted across the thickness of the plate described in the next section.

First let us consider the power-law index $n = 0$ and 1000 as given in Tables 3 and 7. In case of $BaTiO_3$ (piezoelectric), the frequency evaluator using the influence of both the piezo and the magnetic effect (class II) is higher than that of the conventional structural frequency (class I). In contrast, in the case of $CoFe_2O_4$, it is seen that magnetic effect reduces the frequency. This is due to the fact that piezoelectric effect has a tendency to increase the stiffness of the plate by induced electric field, while magnetostrictive material has a tendency to decrease the stiffness of the system by inducing the magnetic field. While in the case of truly sandwich plate (even dominated by magnetostrictive material, e.g $F/B/F$), the combined stiffening effect of piezoelectric and magnetostrictive terms to increase the overall stiffness of the sandwich plate.

From Tables 3–7, it is found that as the value of power-law index increases, the natural frequency decreases as it is approaching toward the homogeneous magnetostrictive material, which corresponds to $n = 1000.0$. It is seen from Tables 3 and 7 that III and II classes of eigenvalues are the same; this is due to the fact that $n = 0$ represents the present plate is fully made up of $BaTiO_3$ only and $n = 1000.0$ corresponds $CoFe_2O_4$ (magnetostrictive) where magneto-electro coupling coefficients are zero. In contrast, for $n = .2$, 1.0 and 5.0, similar behavior is not observed for III and II classes of vibration in Tables 4–6. Further, it is seen that as power-law index n increases, the influence of the magnetic effect is felt more when compared to piezo-electric effect as the material approaches to homogeneous magnetostrictive. This is evidenced by looking at Tables 3–7.

5.2.1. Mode shape variation across the thickness of the FGM magneto-electro-elastic plate for different power-law index

A study has been initiated to look into the thickness mode shape behavior which helps in identifying the appropriate mode where the coupling effect has been felt. Mode shapes corresponding to the appropriate frequencies are plotted across the thickness of the plate for selected power-law index $n = 0$, 1.0 and 10,000. Please note that present study has been carried out on II class of vibration, which takes into account effect of

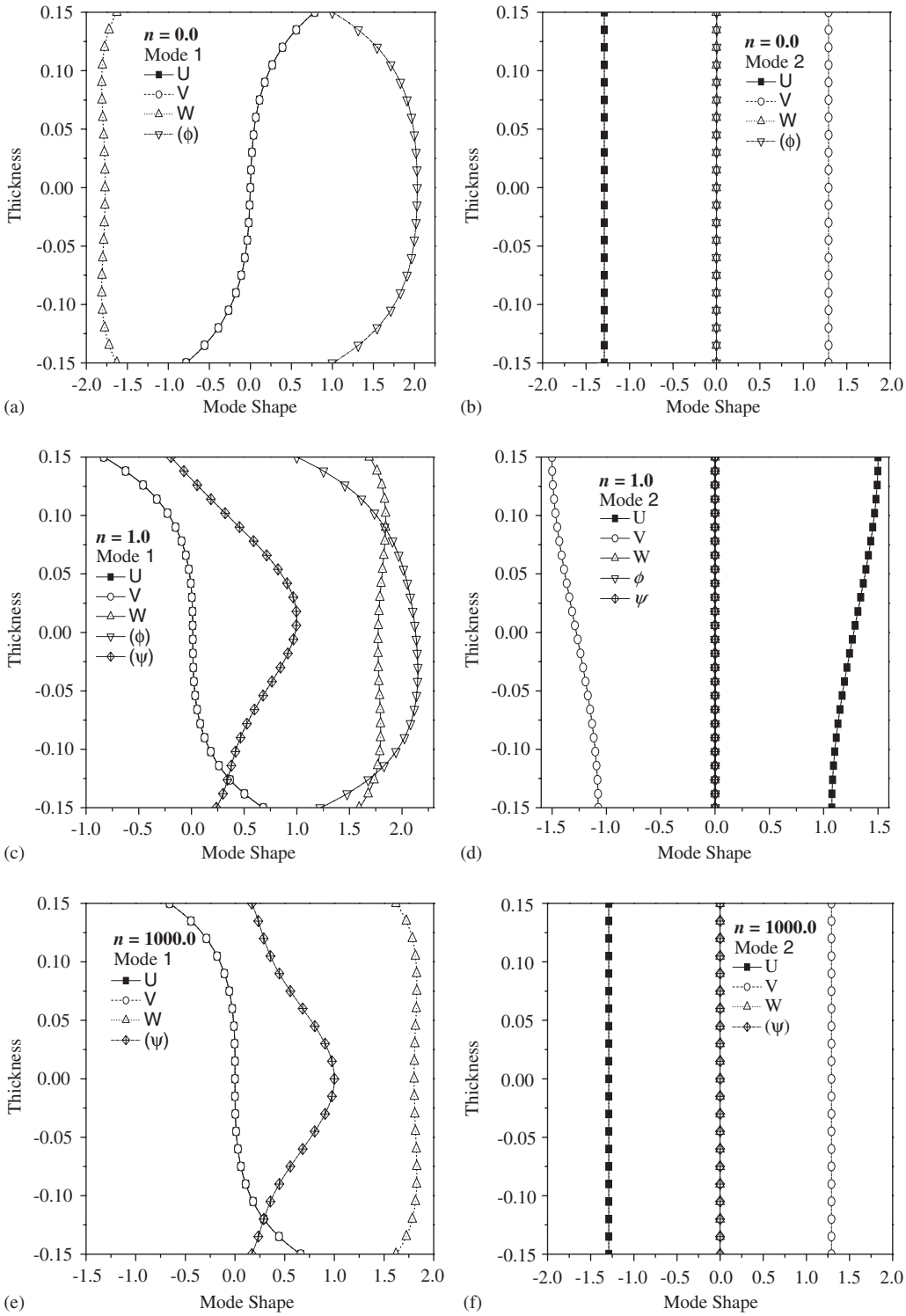

Fig. 4. Symmetric mode shapes for FGM magneto-electro-elastic plate for different power-law index $n = .0$, 1.0 and 1000.0.

magneto-electro-elastic coupling. Fig. 4(a)–(f) shows the symmetric mode shape behavior for the first two modes for different values of the power-law index. Here, frequency belongs to II class of vibration corresponding to mode 1 and 2 as shown in Tables 3, 5 and 7. Let us consider the discussion on mode 1. From Fig. 4(a), it is seen that for $n = 0$ (pure $BaTiO_3$), the transverse displacement which, indicates the bending frequency mode is predominant as compared to inplane elastic displacement. And effect of piezoelectric has been clearly felt by seeing the variation of magnitude of electric potential across the thickness. Similar behavior has been observed for $n = 1000$ (pure $CoFe_2O_4$ magnetostrictive), where electric potential is replaced by magnetic potential as shown in Fig. 4(e). While in case of $n = 1.0$ as shown in Fig. 4(c), where the variation of the piezoelectric and magnetostrictive composition is linear, the variation of the electric as well as magnetic potential across the thickness of the plate along with transverse displacement is shown.

Fig. 4(b), (d) and (e) shows another set of symmetric mode shape corresponding to the frequencies of mode 2. Here, inplane displacements are constant and predominant as compared to transverse displacement, electric potential and magnetic potential. While in case of $n = 1.0$ inplane displacements varies across the thickness and predominant as compared to others. W, electric and magnetic potential vanishes for B only ($n = 0$), $n = 1.0$ and F only ($n = 1000$) cases, which indicates that mode 2 is purely elastic mode and that no effect has been felt of piezoelectric and magnetostrictive coupling.

Fig. 5(a), (c) and (e) shows the antisymmetric mode shape for the corresponding frequencies belonging to the II class of vibration of mode 3 where bending effect is predominant as compared to inplane effect. This material shows clearly the effect of material properties in terms of electric and magnetic potential variation across the thickness. In case of $n = 1.0$, we can see the presence of electric and magnetic potential and their variation in opposite sense. This important feature will not exist in conventional isotropic plate. This gives the freedom in designing for a particular application.

Another set of antisymmetric mode shapes for the corresponding frequencies belonging to II class of vibration of the mode 4 is shown in Fig. 5(b), (d) and (f) . Even though transverse displacement is zero, still some amount of electric and magnetic potential exists along with dominant inplane elastic displacement across the thickness of the FGM plate. It is concluded that even though the frequency mode is insensitive to the coupling effect, still the corresponding mode shows the electric and magnetic potential.

5.2.2. *Numerical studies on FGM (I) plate for higher harmonic modes*

As pointed out, earlier study carried out by Pan and Heyliger [4] and Chen et al. [20] is limited to $m = n = 1.0$. It is felt that even though fundamental mode may be of practical importance, it is possible that there are systems in which higher mode system can be excited. Hence, in the present study, the results are obtained for higher mode also.

Listed in Table 8 are some of the lower eigenvalues (or natural frequencies) for different higher modes for power-law index $n = 1.0$.

As observed in the fundamental harmonic mode, in case of higher harmonic, the frequency evaluator using the influence of both the piezo and the magnetic effect (class II) is higher than that of the conventional structural frequency (class I) and certain of the modes are purely elastic. It is noticed that the first uncoupled elastic mode changes the position for higher harmonic.

Further study has been carried out on different combination of m and n, and only coupled modes are identified and reported in Table 9. As expected similar to elastic system here also mode (1,2) = (2,1), etc. Similar behavior is also observed in higher combination of m and n.

5.2.3. *Studies on FGM magneto-electro-elastic plate with different h/a for open and closed circuit condition*

Study has been carried out on frequency variation for open and closed circuit condition for functionally graded plate. Here, the results obtained by finite element analysis are validated with benchmark solution given by Chen et al. [20]. It is seen that the present formulation has exact correlation with analytical solution mentioned above. Fig. 6(a) shows the variation of the lowest dimensionless frequency with the different power-law index n for I class of vibration. As expected that I class of the frequency depend on the elastic property of the FGM plate, there would not be any effect on closed circuit boundary condition. Further, as we increase the power-law index, composition of the FGM will vary from the pure $BaTiO_3$ to homogeneous $CoFe_2O_4$. Fig. 6(b) shows the two frequency curves belonging to II class of vibration for opened and closed

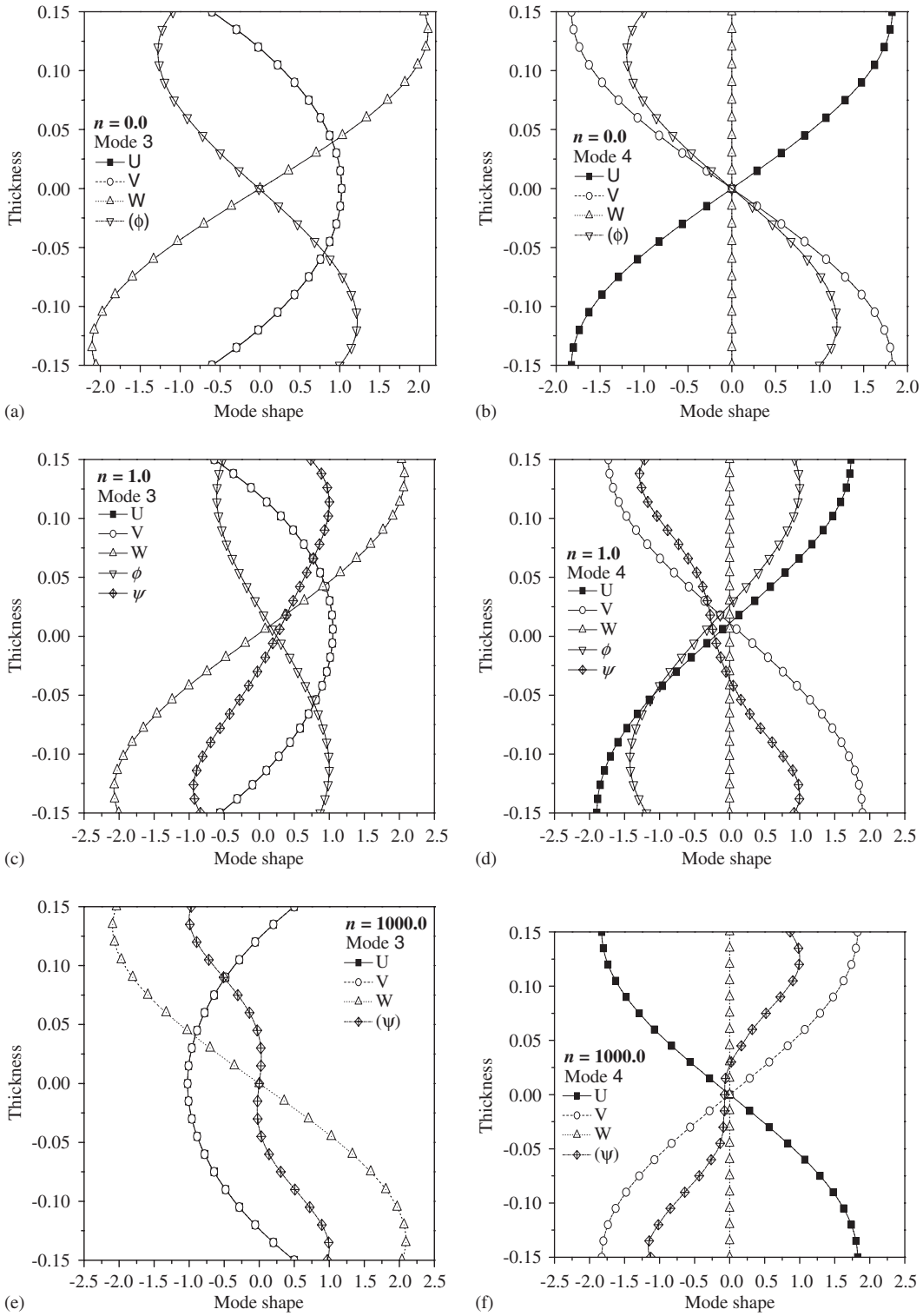

Fig. 5. Antisymmetric mode shape for FGM magneto-electro-elastic plate for different power-law index $n = .0$, 1.0 and 1000.0.

Table 8
Higher harmonic studies for power-law index $n = 1.0$ for frequencies belongs to II class of vibration $\omega^* = \omega L_x\sqrt{C_{\max}/\rho_{\max}}$

Mode	(n, m)							
	(1,1)		(2,1)		(3,1)		(4,1)	
	I	II	I	II	I	II	I	II
1	1.8946	1.9896	3.1592	3.3287	4.5527	4.8086	5.9657	6.3062
2	***2.3394***	***2.3394***	3.5816	***3.6838***	4.7924	4.9991	6.1599	6.4347
3	2.6934	2.7799	***3.6838***	3.7214	***5.1822***	***5.1822***	***6.7247***	***6.7247***
4	***2.8170***	***2.8170***	***4.0392***	***4.0392***	***5.5156***	***5.5156***	***7.0888***	***7.0888***
5	3.8236	3.8904	4.8381	4.8381	5.9035	6.1015	7.1105	7.4514
6	3.8904	3.9260	4.8516	5.0038	6.1015	6.1434	7.5268	7.5268
7	4.4626	4.5506	5.9409	***5.9531***	***7.0157***	***7.0157***	8.1737	***8.2788***
8	***5.2132***	***5.2132***	***5.9531***	6.0839	7.0692	7.2809	***8.2788***	8.4790
9	5.4319	5.5244	6.8115	6.8976	8.1293	8.1293	9.2400	9.2400
10	5.7739	5.8161	7.2329	7.2329	8.1913	8.3888	9.3249	9.5979

Table 9
Higher harmonic studies for power-law index $n = 1.0$ for frequencies belongs to II class of vibration $\omega^* = \omega L_x\sqrt{C_{\max}/\rho_{\max}}$

(n, m)	Order of frequencies				
	Mode 1	Mode 2	Mode 3	Mode 4	Mode 5
(1,1)	1.98968	2.77998	3.92602	4.55060	5.21328
(1,2)	3.32873	3.72145	5.00388	6.08391	6.89769
(1,3)	4.80865	4.99911	6.14341	7.28093	8.38885
(1,4)	6.30627	6.43473	7.45142	8.47900	9.59792
(2,1)	3.32873	3.72145	5.00388	6.08391	6.89769
(2,2)	4.27885	4.52199	5.71977	6.87067	7.92274
(2,3)	5.50447	5.65157	6.73160	7.82599	8.95753
(2,4)	6.84036	6.97251	7.95340	8.93271	10.0302
(3,1)	4.80865	4.99911	6.14341	7.28093	8.38885
(3,2)	5.50447	5.65157	6.73160	7.82599	8.95753
(3,3)	6.49013	6.61824	7.62204	8.63314	9.74555
(3,4)	7.64379	7.79391	8.73297	9.63951	10.6946
(4,1)	6.30627	6.43473	7.45142	8.47900	9.59792
(4,2)	6.84036	6.97251	7.95340	8.93271	10.0302
(4,3)	7.64379	7.79391	8.73297	9.63951	10.6946
(4,4)	8.64131	8.82298	9.72901	10.5510	11.5455

circuit boundary condition. It is noticed that difference between two frequencies for the two electric conditions also varies with power-law index n. Effect is most significant for homogeneous $BaTiO_3$ plate, while the difference decreases with increasing towards homogeneous $CoFe_2O_4$ plate. This is similar to the conclusion reported in Ref. [20].

Further study has been carried on the free vibration of the above FGM plate with $L_x = L_y = 1.0$ for different values of h/L_x for selective power-law index $n = 0$, 1.0 and 1000.0. Results are presented here for open electric circuit condition for II class of vibration. Fig. 7 shows the variation of the non-dimensional frequency for different thickness-to-span ratios for power-law index n. As $h/L_x(h/a)$ ratio decreases, the frequency reduces as the plate become thinner as expected. The difference between frequencies of power-law index was felt in thick plates.

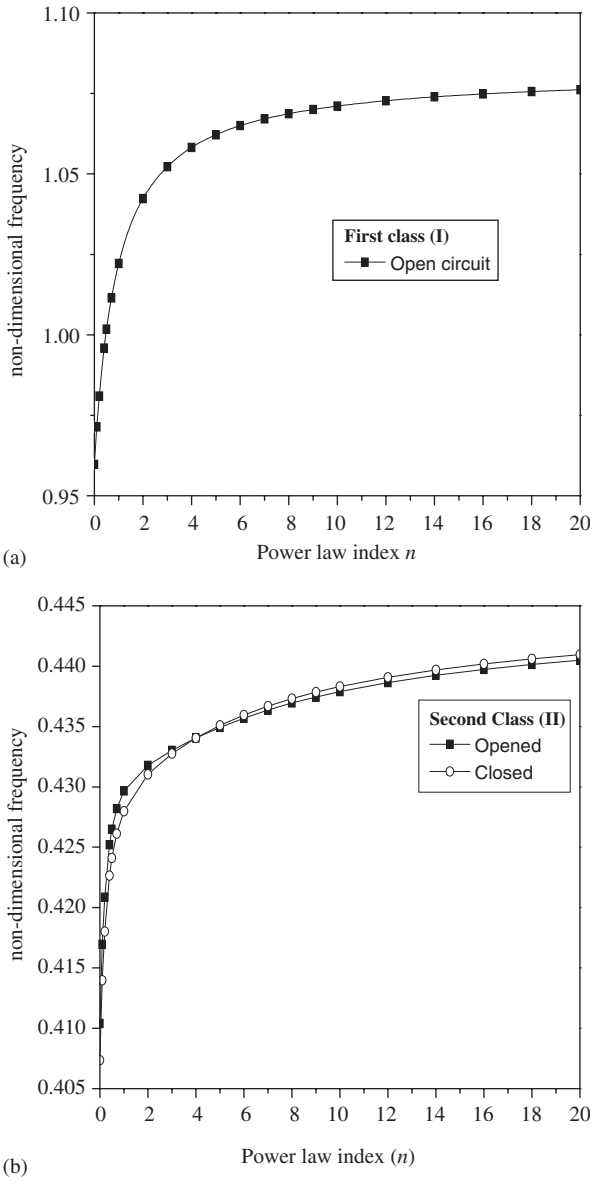

Fig. 6. Variation of the lowest non-dimensional frequency versus the power-law index n (a) I class and (b) II class.

5.3. Studies on functionally graded layered plate (Model-II)

Study has been carried out on functionally graded layered plate having stacking sequences $B/F/B$ and $F/B/F$ with $a = b$ for different values of exponential factor $\eta = 1, -5, 0, +5$ and $+10$. Exponential factor $\eta = 0$ corresponds to the conventional homogeneous sandwich plate made up of $B/F/B$. Tables 10 and 11 gives the first two class of vibration for different exponential factors for FGM-layered plate having stacking sequences $B/F/B$ and $F/B/F$. Please note that the modes that are reported in the subsequent table are actually identified as the coupled modes among the first 11 modes where the coupling effect has been felt. It is seen from table that as exponential factor increases, the frequencies increases. Further, it is seen that the $F/B/F$ stacking sequence has more natural frequencies as compared to $B/F/B$. This is because elastic constants of F ($CoFe_2O_4$) are higher as compared to B ($BaTiO_3$) counterpart.

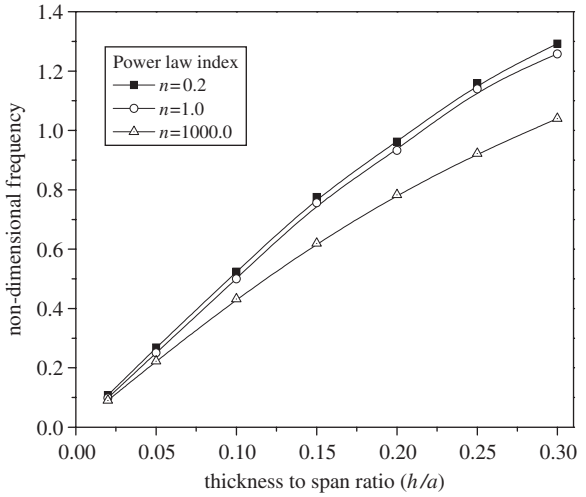

Fig. 7. Variation of the lowest non-dimensional frequency versus thickness to span ratio for different power-law index n.

Table 10
FGM sandwich layered plate (Model II) having stacking sequence $B/F/B$ with different exponential factor for II class of vibration (open circuit)

Mode number	Exponential factor				
	$\eta=-10$	$\eta=-5$	$\eta=0$	$\eta=+5$	$\eta=+10$
1	3.42579	3.69638	3.99075	4.30947	4.65434
2	3.97078	4.32389	4.70578	5.12021	5.56455
3	4.51718	5.01286	5.55968	5.96521	6.14188
4	5.45019	5.62996	5.79793	6.17285	6.86818
5	6.62044	7.27383	7.93486	8.55374	9.22177
6	6.77719	7.34506	7.95529	8.66595	9.39054
7	6.83669	7.80587	8.88309	10.08562	11.42305
8	8.89069	9.73966	10.61499	11.50556	12.40378
9	8.97736	10.11918	11.33044	12.58028	13.04328
10	10.92316	11.56499	12.12140	12.63030	13.94953
11	11.39735	12.45568	13.53852	14.64553	15.77345

Table 11
FGM sandwich layered plate (Model II) having stacking sequence $F/B/F$ with different exponential factor for II class of vibration (open circuit)

Mode number	Exponential factor				
	$\eta=-10$	$\eta=-5$	$\eta=0$	$\eta=+5$	$\eta=+10$
1	3.640610	3.874117	4.136890	4.434772	4.773940
2	4.150271	4.515321	4.902647	5.310984	5.732444
3	4.819158	5.368926	5.804609	5.958868	6.130892
4	5.505962	5.657273	5.974930	6.650351	7.406637
5	6.786809	7.393943	8.039491	8.735699	9.506848
6	6.826690	7.590555	8.325885	9.019294	9.667535
7	7.309885	8.435417	9.664533	10.966288	11.846675
8	9.041019	9.894806	10.780147	11.630464	12.319095
9	9.282835	10.412854	11.374247	11.688902	12.618292
10	10.745510	11.086944	11.710422	13.165133	14.712670
11	11.551625	12.613866	13.700462	14.814165	15.955190

5.4. Studies on layered plate with different h/a with open and closed electric circuit conditions

Study has been carried out for FGM sandwich plate for frequency variation under the influence of open and closed circuit condition. Fig. 8 shows the variation of the lowest dimensionless frequency with the different values of exponential factor η for II class of vibration for mode 1. Fig. 8(a) shows the two frequency curve belonging to open and closed circuit boundary conditions. It is noticed that difference between two frequencies for the two electric conditions increases when there is an increase in exponential factor η. This is because the exponential factor $\eta = +10$ has more amount of $BaTiO_3$ on top surface. In contrast, Fig. 8(b) shows the negligible effect of closed circuit boundary condition on FGM sandwich plate $F/B/F$. This behavior can be explained by looking, the properties of $CoFe_2O_4$ where piezoelectric coupling coefficients are zero.

Study has been carried out on two stacking sequences namely $B/F/B$ and $F/B/F$ sandwich plate with $a = b$ for different values of h/a. Tables 12 and 13 give the first two classes of vibration for different h/a for selective exponential factor $\eta = +10$. Once again note that the modes that are reported in the subsequent table are

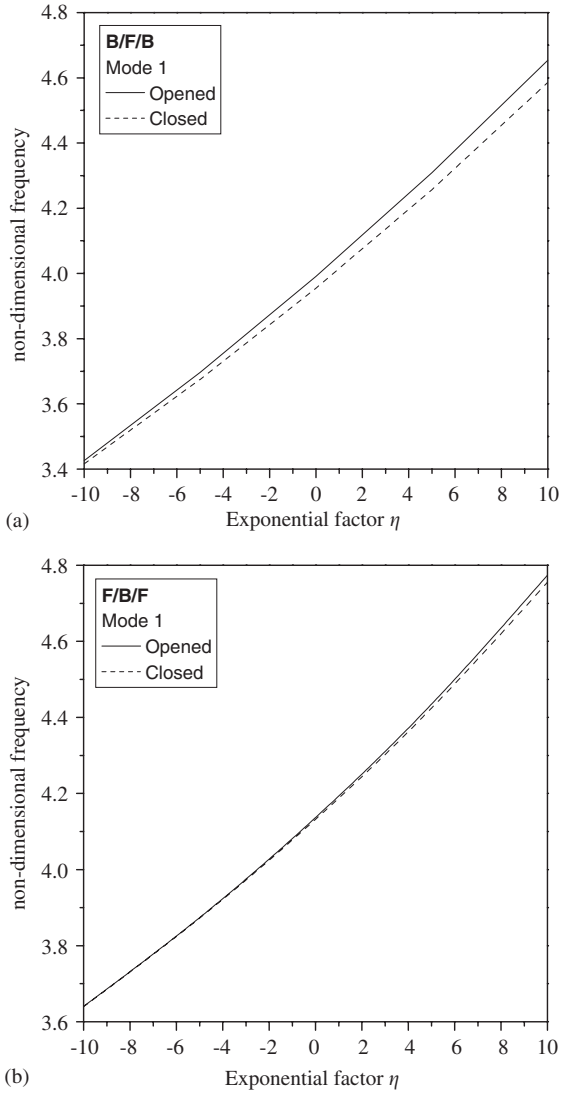

Fig. 8. Variation of the lowest non-dimensional frequency versus the exponential factor for open and closed circuit conditions: (a) $B/F/B$ sandwich plate and (b) $F/B/F$ sandwich plate.

Table 12
Natural frequency $\Omega = \omega h\sqrt{\rho/C_{44}}$ belongs to II class of vibration of a square plate for different thickness to span ratio (h/a) for $B/F/B$ sandwich plate having exponential factor $\eta = +10$ with open circuit and closed circuit

h/a	Class	Frequency order				
		Mode 1	Mode 2	Mode 3	Mode 4	Mode 5
.5	I	3.24651	5.01787	8.27823	12.40097	16.40447
	II	*2.20103*	*4.65092*	*6.99546*	*8.25791*	*10.43482*
		(2.17167)	(4.64865)	(6.98185)	(8.23132)	(10.27387)
.3	I	1.69534	3.80197	7.32924	11.17946	14.85336
	II	*.93802*	*2.90250*	*4.67285*	*6.94900*	*8.94816*
		(.93040)	(2.90243)	(4.60888)	(6.81623)	(8.73884)
.2	I	1.05811	3.47439	6.95564	10.60514	14.11456
	II	*.44064*	*1.85862*	*3.92045*	*6.85770*	*8.27079*
		(.43845)	(1.85817)	(3.82730)	(6.65376)	*(8.08718)*
.1	I	.49806	3.28464	6.62181	10.04917	13.39841
	II	*.11072*	.88344	*3.46280*	*6.78329*	*7.65276*
		(.11065)	(.88314)	(3.39145)	(6.53858)	*(7.57697)*
.05	I	.24220	3.22840	6.46584	9.77578	13.04873
	II	*.02702*	*.43039*	*3.34396*	*6.58444*	*7.42068*
		(.02702)	(.43025)	(3.25272)	(6.44598)	*(7.40347)*
.02	I	.09535	3.20414	6.37506	9.61735	12.84158
	II	*.00422*	*.16952*	*3.30552*	*6.40245*	*7.33483*
		(.00422)	(.16946)	(3.20789)	(6.37208)	(7.32971)

Table 13
Natural frequency $\Omega = \omega h\sqrt{\rho/C_{44}}$ of a square plate for different thickness to span ratio (h/a) for $F/B/F$ sandwich plate having exponential factor $\eta = +10$ with open circuit and closed circuit

H/a	Class	Mode 1	Mode 2	Mode 3	Mode 4	Mode 5
.5	I	3.460057	5.298218	8.419655	12.528745	16.476629
	II	*2.320855*	*4.665851*	*7.610018*	*8.431468*	10.022958
.3	I	1.805288	3.878484	7.422588	11.279991	14.907517
	II	*1.014523*	*3.041130*	*5.057818*	*6.876614*	8.393655
.2	I	1.120203	3.491665	7.048815	10.698564	14.169584
	II	*.484493*	*1.958711*	*4.169641*	*6.675129*	7.768470
.1	I	.523248	3.272736	6.719636	10.136980	13.459274
	II	*.123356*	*.927858*	*3.615219*	*6.657661*	7.322505
.05	I	.253371	3.211526	6.566482	9.863213	13.114104
	II	*.030208*	*.030208*	*3.466236*	*6.543709*	7.121635
.02	I	.099488	3.186796	6.477342	9.701247	12.910113
	II	*.004724*	*.176949*	*3.415383*	*6.477342*	7.060414

coupled modes identified among the first 11 modes. Open and closed circuit condition is assumed at the top and bottom surface of the plate. In bracket frequency value depicts the closed circuit condition widely used terminology in the smart structure. Italic notations are used for the effect of coupling of magneto-electro-elastic structures. While parenthesis frequencies indicate the effect of closed circuit boundary conditions.

From Table 12, it is visible that frequencies for the closed circuit conditions are usually lower than the corresponding open circuit condition. Since the I class of vibration depends upon the elastic property of the system, the electric boundary condition on the plate surface does not affect the associated frequency. It is seen from Table 12 that increase in h/a ratio causes the frequencies decrease as the plate become thinner, as expected. Important observation from Tables 12 and 13 is that as the thickness of the plate decreases, the gap between numerical values of I (inplane mode) and II (bending mode) class of vibration increases. Even then, it is found that the influence of magneto-electro-elastic coupling is felt on bending frequencies (II class of vibration). The $F/B/F$ stacking sequence has more natural frequencies as compared to $B/F/B$. This is due to the fact that elastic constants of F ($CoFe_2O_4$) are higher as compared to B ($BaTiO_3$) counterpart. Effect of closed circuit condition on $F/B/F$ stacking sequence is felt less. This may be due to the fact that both top and bottom surfaces have F-only plate where piezoelectric coupling term vanishes.

6. Conclusion

In this article, finite element procedure is adopted for the vibration of the 3-D, anisotropic, magneto-electro-elastic plate. A series solution is assumed in the plane of the plate and finite element procedure is adopted across the thickness direction. The present solution is a natural extension of the corresponding static solution for FGM plates developed recently by authors [14]. The model is derived based on constitutive equation of magneto-electro-elastic material. Coupling between elasticity, electric and magnetic effects are included in the analysis. The FGM plate is graded in the thickness direction and a simple power-law index will govern the magneto-electric constituents profile across the thickness. It is found that different exponential factors in functionally graded (Model-I) and functionally graded and layered plate (Model-II) shows the different vibration characteristics. The results of the present model are in good agreement with the exact benchmark solution for magneto-electro-elastic plate given by Pan and Heyliger [4] and Chen et al. [20]. Following are the conclusions arrived:

(1) As power-law index increases, the frequency decreases as the constituent of material reaches homogeneous magnetostrictive material for FGM model 'I'; while in case of FGM model 'II', the frequencies increases as exponential factor increases.
(2) It is found that some of the vibration modes in purely elastic media are insensitive to the coupling of magneto-electro-elastic. But at higher modes, they still can produce electric and magnetic potentials.
(3) In general, the piezoelectric effect has the tendency of stiffening the plate and hence, increases the structural natural frequency. In contrast, pure magnetic effect has a negative influence on the system frequency and reduces the structural natural frequency marginally.
(4) While FGM-layered magneto-electro-elastic plate for both stacking sequences ($B/F/B$ and $F/B/F$) increase the frequency of the structure. This is due to the fact that overall stiffness of the system increases because of the internal forces generated by induced electric and magnetic field and dominance effect of piezoelectric.
(5) For the piezoelectric/magnetostrictive coupling mode, all the mode shapes, especially elastic displacements component and electric and magnetic potential strongly depends on material composition of the magneto-electro-elastic plate governed by different power-law indices.
(6) Power-law index other than two extreme ends produces both electric as well magnetic potentials, which otherwise is absent in single monolithic components.
(7) Effect of open and closed circuit electric boundary conditions is felt more for piezoelectric-dominated grading region as compared to magnetostrictive where the piezoelectric coupling vanishes.
(8) As the thickness of the plate decreases, the gap between numerical values of I (inplane mode) and II (bending mode) class of vibration increases. Even then, it is found that influence of magneto-electro-elastic coupling is felt on bending frequencies (II class of vibration).

The advantage of functionally graded material model over the layered model is that there is no discontinuity between the electric, magnetic potential between the layers. It is felt that the present numerical study is highly useful for characterizing FGM magneto-electro-elastic system for use as sensors or actuators.

Appendix

Material coefficients of the magneto-electro-elastic plate

	$CoFe_2O_4$	$BaTiO_3$
C_{11}	286	166
C_{12}	173	77
C_{13}	170	78
C_{33}	269.5	162
C_{44}	45.3	43
e_{15}	0	11.6
e_{31}	0	−4.4
e_{33}	0	18.6
ε_{31}	.08	11.2
ε_{33}	.093	12.6
μ_{11}	−5.9	.05
μ_{33}	1.57	.1
q_{15}	560	0
q_{31}	580	0
q_{33}	700	0
m_{11}	0	0
m_{33}	0	0

C_{ij} in $10^9\,N/m^2$, e_{ij} in C/m^2, ε_{ij} in $10^{-9}\,C/V\,m$, q_{ij} in $N/(A\,m)$, μ_{ij} in $10^{-4}\,N\,s^2/C^2$, m_{ij} in $10^{-9}\,N\,s/V\,C$.

References

[1] G. Harshe, J.P. Dougherty, R.E. Newnham, Theoretical modeling of multilayered magnetoelectric composites, *International Journal of Applied Electromagnetic in Materials* 4 (1993) 145–159.

[2] C.W. Nan, Magnetoelectric effect in composites of piezoelectric and piezomagnetic phases, *Physics Review B* 50 (1994) 6082–6088.

[3] E. Pan, Exact solution for simply supported and multilayered magneto-electro-elastic plates, *Journal of Applied Mechanics, ASME* 68 (2001) 608–618.

[4] E. Pan, P.R. Heyliger, Free vibrations of simply supported and multilayered magneto-electro-elastic plates, *Journal of Sound and Vibration* 252 (2002) 429–442.

[5] X. Wang, Z. Zhong, A finitely long circular cylindrical shell of piezoelectric/ piezomagnetic composite under pressuring and temperature change, *International Journal of Engineering Science* 41 (2003) 2429–2445.

[6] J. Aboudi, Micromechanical analysis of fully coupled electro-magneto-thermo-elastic multiphase composites, *Smart Materials and Structures* 10 (2001) 867–877.

[7] J.Y. Li, Magnetoelectroelastic multi-inclusion and inhomogeneity problems and their applications in composite materials, *International Journal of Engineering Science* 38 (2000) 1993–2011.

[8] J. Wang, L. Chen, S. Fang, State vector approach to analysis of multilayered magneto-electro-elastic plates, *International Journal of Solids Structures* 40 (2003) 1669–1680.

[9] G.R. Buchanan, Free vibration of an infinite magneto-electro-elastic cylinder, *Journal of Sound and Vibration* 268 (2003) 413–426.

[10] G.R. Buchanan, Layered verses multiphase magneto-electro-elastic composites, *Composites B (Engineering)* 35 (2004) 413–420.

[11] G.R. Lage, C.M. Soares, C.A. Soares, J.N. Reddy, Layer wise partial mixed finite element analysis of magneto-electro-elastic plates, *Computers and Structures* 76 (2004) 299–317.

[12] R.K. Bhangale, N. Ganesan, Free vibration of functionally graded non-homogeneous magneto-electro-elastic cylindrical shell, International Journal of Computational Science in Engineering and Mechanics, 2005, in press.

[13] R.K. Bhangale, N. Ganesan, Free vibration studies of simply supported non-homogeneous functionally graded magneto-electro-elastic finite cylindrical shells, *Journal of Sound and Vibration* 288 (2005) 412–422.

[14] R.K. Bhangale, N. Ganesan, Static analysis of functionally graded and layered magneto-electro-elastic plate, *International Journal of Solids Structures*, 2005, in press.

[15] E. Pan, Exact solution for functionally graded anisotropic elastic composite laminates, *Journal of Composite Materials* 37 (2003) 1903–1920.
[16] E. Pan, F. Han, Green's function for transversely isotropic piezoelectric functionally graded multilayered half spaces, *International Journal of Solids Structures* 42 (2004) 3207–3233.
[17] R.K. Bhangale, N. Ganesan, A linear thermoelastic buckling analysis of functionally graded hemispherical shell with cut-out at apex, *International Journal of Structural Stability and Dynamics* 5 (2005) 185–215.
[18] R.K. Bhangale, N. Ganesan, A linear thermoelastic buckling and free vibration analysis of functionally graded truncated conical shell, *Journal of Sound and Vibration* 292 (2005) 341–371.
[19] W.Q. Chen, K.Y. Lee, Alternative state space formulations for magneto electric thermo elasticity with transverse isotropy and the application to bending analysis of nonhomogeneous plate, *International Journal of Solids Structures* 33 (2003) 977–990.
[20] W.Q. Chen, K.Y. Lee, H.J. Ding, On free vibration of non-homogeneous transversely isotropic magneto-electro-elastic plates, *Journal of Sound and Vibration* 279 (2005) 237–251.
[21] E. Pan, F. Han, Exact solution for functionally graded and layered magneto-electro-elastic plates, *International Journal of Engineering Science* 43 (2005) 321–339.